The influence of lithospheric thickness variations beneath Australia on seismic anisotropy and mantle flow

C.M. Eakin [1*], D.R. Davies [1], S. Ghelichkhan [1], J.P. O'Donnell [2†], S. Agrawal [1]

[1] Research School of Earth Sciences, The Australian National University, Canberra, ACT, Australia

[2] Geological Survey of South Australia, Department for Energy and Mining, Adelaide, SA, Australia

[*] Corresponding author: Caroline M. Eakin (caroline.eakin@anu.edu.au)

[†] Now at Geological Survey of Western Australia, Perth, WA, Australia

Key Points:

- Fossilized anisotropy dominates where lithosphere is old and thick, with deformation of the Gawler Craton from ~1.6 Ga preserved
- Asthenospheric shear relating to Australia's fast plate motion dominates where lithosphere is young and thin
- Lithospheric thickness variations likely induce further deviations in mantle flow

Abstract

Rapid plate motion, alongside pronounced variations in age and thickness of the Australian continental lithosphere, make it an excellent location to assess the relationship between seismic anisotropy and lithosphere-asthenosphere dynamics. In this study, SKS and PKS shear-wave splitting is conducted for 176 stations covering the transition from the South Australian Craton to eastern Phanerozoic Australia. Comparisons are made with models of lithospheric thickness as well as numerical simulations of mantle flow. Splitting results show uniform ENE-WSW aligned fast directions over the Gawler Craton and broader South Australian Craton, similar to the orientation of crustal structures generated during an episode of NW-SE directed compression and volcanism ~1.6 billion years ago. We propose that heat from volcanism weakened the lithosphere, aiding widespread lithospheric deformation, which has since been preserved in the form of frozen-in anisotropy. Conversely, over eastern Phanerozoic Australia, fast directions show strong alignment with the NNE absolute plate motion. Overall, our results suggest that when the lithosphere is thin (<125 km), lithospheric contributions are minimal and contributions from asthenospheric anisotropy dominate, reflecting shear of the underlying mantle by Australia's rapid plate motion above. Further insights from geodynamical simulations of the regional mantle flow-field, which incorporate Australian and adjacent upper mantle structure, predict that asthenospheric material would be drawn in from the south and east towards the fast-moving continental keel. Such a mechanism, alongside interactions between the flow field and lithospheric structure, provides a plausible explanation for smaller-scale anomalous splitting patterns beneath eastern Australia that do not align with plate motion.

Plain Language Summary

The Australian continent is moving rapidly northwards at around 7-8 cm per year. As the continent moves it is expected to shear or deform the warmer and weaker layer of the Earth below, called the mantle. The actual pattern of deformation within the mantle can be investigated by studying how seismic waves are polarized as they pass through this material. Results show that for one of the geologically oldest regions in Australia, an area in South Australia, that the deeper part of the continent here was substantially deformed 1.6 billion years ago. This deformation was likely aided by volcanism that occurred at the same time that would have warmed and weakened the material making it easier to deform. This material has since cooled and strengthened over time, freezing in

the ancient pattern of deformation. Meanwhile in eastern Australia, the continental material here has a much younger geological age (< 550 million years old). The results from this region instead show agreement with the present-day direction of shear due to the fast northwards motion of the Australian continent, as initially expected.

1 Introduction

Seismic anisotropy, the directional dependence of seismic wave velocity, is a powerful property for studying dynamic processes within Earth's interior. When the upper mantle undergoes deformation in the dislocation creep regime, a lattice preferred orientation, (i.e. LPO fabric), is expected to develop in olivine (Nicolas and Christensen, 1987). Under typical upper mantle conditions the fast a-axes of olivine will tend to align with the direction of shear (e.g. Karato et al., 2008; Zhang and Karato, 1995) . Using seismic waves that pass through the upper mantle, the geometry and strength of anisotropy can be measured, and inferences drawn on the pattern of mantle flow. Seismic anisotropy, therefore, provides an excellent observation-based constraint on mantle convection, particularly for investigations of the relationship between surface plate kinematics and underlying mantle dynamics.

Investigations of upper mantle dynamics via seismic anisotropy are, however, not without ambiguity. One additional factor to consider is the potential for frozen-in or fossilized anisotropy within lithospheric mantle. The lithosphere, Earth's stiff outermost layer, should not be actively generating LPO. However, observations suggest it may preserve an olivine LPO fabric that developed either during its formation (e.g. at the mid-ocean ridge), or during past tectonic/orogenic events that could generate lithospheric deformation (e.g. Debayle and Ricard, 2013; Silver, 1996). The ability to constrain the pattern of fossilized anisotropy therefore holds great potential for revealing the behavior and evolution of Earth's lithosphere.

The Australian plate provides an excellent testing ground for interactions between seismic anisotropy, mantle dynamics, and the lithosphere-asthenosphere system. Australia is the fastest moving continent on Earth with an absolute plate motion of 7-8 cm per year towards the north-northeast (Kreemer et al., 2014). Such rapid plate motion may exert significant shear on the upper mantle at the base of the tectonic plate (e.g. Debayle et al., 2005). The Australian continental lithosphere also varies substantially both in terms of age and thickness (Figure 1), with likely implications for lithospheric anisotropy.

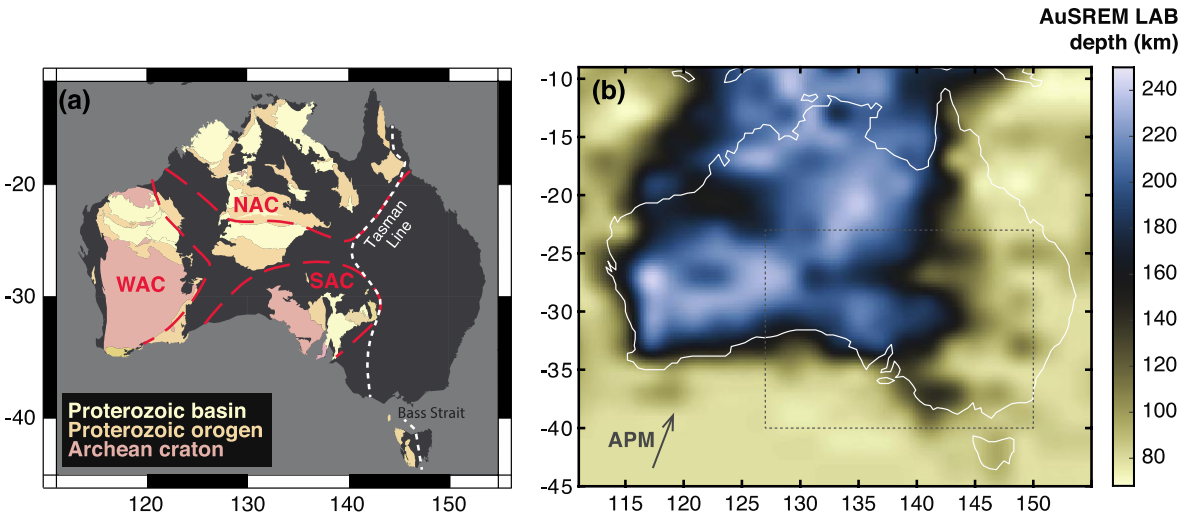

Figure 1. Overview of the Australian continent indicating (a) the location of cratons, and (b) the variation in lithospheric thickness from AuSREM (Kennett et al., 2012). The oldest Precambrian provinces of Australia from Raymond et al., (2018) are highlighted in beige and pink colours in (a). The inferred boundary between Precambrian and Phanerozoic Australia, often referred to as the Tasman Line (Direen and Crawford, 2010), is indicated by the dashed white line. The approximate extent of the West Australian Craton (WAC), North Australian Craton (NAC), and South Australian Craton (SAC) is outlined in red. The dotted grey box in (b) indicates the study area shown in Figures 2-3. The small black arrow represents the absolute plate motion (APM) vector of the Australian plate from Kreemer et al., (2014).

In addition to varying contributions of lithospheric anisotropy, the existence of lithospheric steps and substantial 3D topography on the lithosphere-asthenosphere boundary (LAB) likely induces deviations of the upper mantle flow-field as the uneven basal topography of the plate traverses the underlying asthenosphere (Rawlinson et al., 2017). Small-scale convective flow patterns induced by various LAB geometries can be predicted by geodynamic modelling (Duvernay et al., 2021; Farrington et al., 2010), but remain strongly sensitive to uncertain lithospheric structure and uppermost mantle rheology. Nonetheless a number of recent studies have started to link variations in lithospheric thickness/architecture beneath Australia with important and varied surface processes, including Cenozoic volcanism (Davies and Rawlinson, 2014; Rawlinson et al., 2017), the localization of critical mineral deposits (Hoggard et al., 2020),

dynamic topography (Ball et al., 2021), and intra-plate seismicity (Bezada and Smale, 2019).

Upper mantle anisotropy is typically studied either by surface wave tomography or shear-wave splitting methodologies. Globally the inferences from surface waves and shear-wave splitting tend to agree (Wüstefeld et al., 2009). However, this has not been the case in Australia. Surface wave studies tend to see a strong signal in both azimuthal and radial anisotropy at the base of the continental lithosphere, with fast directions aligned with absolute plate motion (APM) and the expected shear of the underlying asthenosphere (Debayle et al., 2005; Debayle and Ricard, 2013; Fichtner et al., 2010; Fishwick et al., 2008; Simons et al., 2002; Yoshizawa, 2014; Yoshizawa and Kennett, 2015), although not all models agree (e.g. de Laat et al., 2023). Conversely, shear-wave splitting studies using core-refracted phases, such as *SKS*, have typically not detected plate-motion aligned fast directions (e.g. Heintz and Kennett, 2006).

The number of previous shear-wave splitting studies across Australia (~10) is relatively limited compared to other continental landmasses. Previous authors have typically reported either: (i) weak splitting (i.e. many null measurements or small delay times) (Ba et al., 2023; Chen et al., 2021; Eakin et al., 2021; Heintz and Kennett, 2005; Özalaybey and Chen, 1999; Vinnik et al., 1992); (ii) complex patterns such as frequency dependence of the splitting parameters (Clitheroe and van der Hilst, 1998; Özalaybey and Chen, 1999); or (iii) variability of the retrieved splitting parameters at a given station (Bello et al., 2019; Birkey and Ford, 2022; Chen et al., 2021; Heintz and Kennett, 2006, 2005). Various interpretations have been proposed to explain such results, including: (i) a lack of azimuthal anisotropy present in the upper mantle (Chen et al., 2021; Özalaybey and Chen, 1999); (ii) apparent isotropy due to two anisotropic layers with orthogonal fast directions (Heintz and Kennett, 2006); (iii) contributions from frozen-in lithospheric anisotropy but without clear correspondence to structural trends at the surface (Bello et al., 2019; Birkey and Ford, 2022; Clitheroe and van der Hilst, 1998; Heintz and Kennett, 2005); or (iv) the possibility of asthenospheric flow that is not aligned with the APM, such as around a continental root (Ba et al., 2023; Clitheroe and van der Hilst, 1998; Heintz and Kennett, 2005).

Most previous shear-wave splitting studies in Australia had ≤35 stations available, often sparsely distributed on a continental scale, making it difficult to pin-point the cause and location of spatial variations in anisotropy. The first exception is the study of Heintz and Kennett (2005), which had a large number of stations (>100) but was hindered by unusually short recording times

(average <6 months), and, therefore, a restricted number of events. The second exception is a recent study by Ba et al. (2023) who reported shear-wave splitting results from 116 stations across the continent with spatially complex patterns. Unlike previous studies, Ba et al. (2023) were able to identify certain locations, such as the peripheral areas of the continent, where the splitting pattern matched well with the direction of absolute plate motion. Overall, they attributed their results to asthenospheric mantle flow with possible (yet unquantified) lithospheric contributions.

Recent results from the BILBY north-south transect (Eakin et al., 2021), however, identified a clear correspondence between the splitting fast axis and prominent structural/gravity trends across the South and North Australia Cratons, as well as the suture zone in-between. This provided strong evidence that the shear-wave splitting results in this particular cratonic region are predominantly reflecting lithospheric frozen-in anisotropy rather than asthenospheric contributions. All BILBY stations, however, were located on thick cratonic lithosphere, and so the question of variable lithospheric contributions could not be assessed.

In this study we aim to utilize a compilation of over 170 stations that traverse the region extending from thick cratonic lithosphere beneath the South Australia Craton to thinner Phanerozoic lithosphere towards the east. The study is supported by our two recent deployments in South Australia that provide unprecedented coverage of the eastern Gawler margin and South Australian Craton (Eakin, 2019; O'Donnell et al., 2020). Using new data and shear-wave splitting measurements from across these seismic networks we can determine, in detail, how variations in lithospheric thickness and architecture exert a first order control on the pattern of seismic anisotropy and upper mantle dynamics beneath Australia.

2 Tectonic Overview

A large difference in age exists between the western two-thirds of Australia, which is of Precambrian/Proterozoic origin, and the eastern Phanerozoic margin. Precambrian Australia consists of three main crustal components: the North, South, and West Australia Cratons (Figure 1a). These are thought to have existed since ~1.8 Ga and were assembled by 1.3-1.1 Ga, during the Rodinia supercontinent cycle, to form proto-Australia (Betts and Giles, 2006; Myers et al., 1996). In contrast, the eastern third of Australia can be described as a series of accretionary or orogenic belts, added to the eastern margin of proto-Australia during the Cambrian to Triassic

periods (~550-220 Ma) via subduction (e.g. Glen, 2005). The geological boundary demarcating cratonic Precambrian Australia from eastern Phanerozoic Australia is sometimes referred to as the Tasman Line (Direen and Crawford, 2003) (Figure 1). The precise location of the Tasman Line, inferred from various geophysical and geological observations is, however, often poorly constrained, especially in regions of thick sedimentary cover such as beneath the Lake Eyre region (Agrawal et al., 2022). Nonetheless, it is clear from Figure 1b that western Precambrian Australia is generally underlain by thick lithosphere (>150 km), whereas eastern Australia is characterised by relatively thin continental lithosphere, typically ~75 km thick (Fishwick et al., 2008; Kennett and Salmon, 2012).

Our study area covers most of the South Australian Craton, the core of which is composed of the Archean-Proterozoic Gawler Craton and the Proterozoic Curnamona Province (Figures 1-2). The Gawler Craton is the oldest and largest geological province in South Australia and preserves a complex tectonic history spanning from 3200 Ma to 1450 Ma (Myers et al., 1996). The Archean and Paleoproterozoic core of the Gawler Craton forms a folded belt that underwent deformation along discrete shear zones during the Mesoproterozoic (Hand et al., 2007). Throughout the Proterozoic, the region saw multiple major magmatic events, recorded in the geological record by the Donington Suite (ca. 1850 Ma), St. Peter Suite (1620 to 1610 Ma), and Gawler Range Volcanics-Hiltaba Suite (1595 to 1575 Ma) (Hand et al., 2007).

3 Data and Methods

3.1 Station and event availability

In total 176 stations in Australia were analysed for *SKS* and *PKS* splitting in this study. The distribution of these stations covers a wide area including the South Australia Craton (Gawler and Curnamona Provinces), as well as Phanerozoic regions to the east and south-east (Figure 2a). Two new seismic deployments in South Australia provide increased station coverage over the eastern Gawler Craton (yellow and green symbols in Figure 2a). The first of these deployments is the Lake Eyre Basin Seismic Array (Network: 5G), including 22 broadband stations deployed in the region surrounding Kati Thanda-Lake Eyre (Eakin, 2019). Instruments were installed in several phases between September 2018-October 2019, and remained in-place until July 2022. Several data gaps exist, including the period from June-October 2020 resulting from COVID-19 related state border

closures and travel restrictions that prevented servicing of the network. A second array, AusArray-SA (Network: 6K), was deployed south of the Lake Eyre Basin array by the Geological Survey of South Australia (O'Donnell et al., 2020). This consisted of 38 broadband stations that operated over a similar timeframe from October 2020 to June 2022.

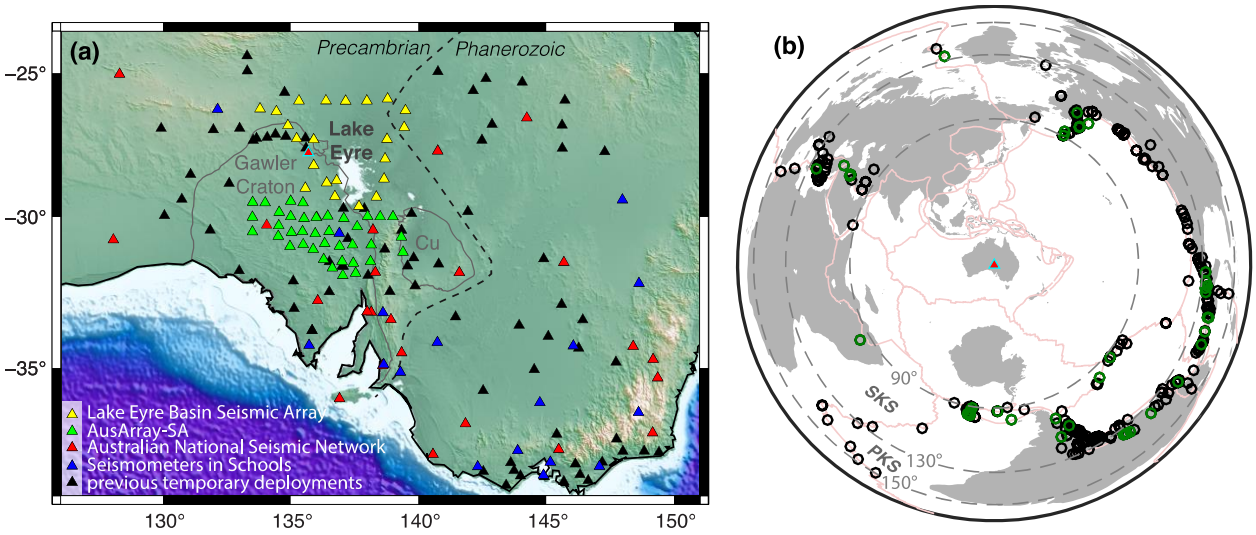

Figure 2. Map showing distribution of (a) seismic stations, and (b) earthquakes used in this study. The dashed black line in (a) indicates the approximate position of the Tasman Line for this region. The outline of the Gawler Craton and Curnamona (Cu) province are shown in grey. The event map presented in (b) shows the typical event distribution at one station, OOD, the location of which is highlighted in (a) in cyan. Events are plotted as open circles colour-coded by those that produced a splitting measurement (green), and those that did not (black).

The station coverage is supplemented by data from two permanent national networks. These include 23 stations from the Australia National Seismic Network (red symbols in Figure 2a, Network: AU) and 17 stations from the Australian Seismometers in Schools (AuSiS) program (blue symbols Figure 2a, Network: S1). The remaining 76 stations (black symbols) represent a compilation of 8 past temporary broadband deployments. Most of these sites operated for 12-24 months. A full list of all temporary (and permanent) networks is provided in the data availability section. The majority of these sites have not been previously analysed for *SKS* splitting. Those that

have are re-analysed to ensure consistency in the methodology across the region. The only exceptions are results from the BILBY array (stations BL:15, 16, 17, 19, 20, 24) and permanent station AU:MULG from our earlier study of Eakin et al., (2021). This study followed the same methodology as is applied here and therefore these results are directly included in the dataset without re-processing.

For event selection, earthquakes of magnitude 6.0 and above were utilised in the epicentral distance range 90°-130° for *SKS* and 130°-150° for *PKS* phases (Figure 2b). This equates to around 30-40 events per year for a seismic station in southern Australia. While events originate across a range of backazimuths they are most plentiful from the South America subduction zone from the south-southeast direction (Figure S4).

3.2 Shear-wave splitting processing and methodology

Shear-wave splitting analysis was undertaken using the SplitLab software package (Wüstefeld et al., 2008). Multiple methods for estimating the best-fitting shear-wave splitting parameters (the fast direction: Φ and delay time: δt) are available within the SplitLab environment. For quality control purposes we compare estimates from two independent methods. The first is the rotation correlation (RC) method (Bowman and Ando, 1987), which determines the values of Φ and δt, which generate the maximum cross-correlation between the trial fast and slow components. This method can produce systematic error as a function of initial polarisation, or as a function of backazimuth for **KS* phases (Eakin et al., 2019; Wüstefeld and Bokelmann, 2007). When the initial polarisation approaches the fast or slow orientation of the anisotropic medium the RC method will predict a best fitting value of Φ that deviates 45° from the true value, with a delay time that is close to zero (e.g. Figure S9). While such systematic measurement error is not ideal, it is well understood and predictable. With this in mind, the true splitting parameters can still be easily retrieved from this method (Eakin et al., 2019).

The second method is the transverse energy minimisation (SC) method (Silver and Chan, 1991). Using this method, we seek those values of Φ and δt that best minimise the energy on the transverse component, following a correction for shear-wave splitting. The SC

method is thought to produce more stable *SKS* splitting measurements over a wider range of backazimuths. However, it can also be susceptible to the same systematic error as seen for the RC method when the signal-to-noise ratio is moderately high (Eakin et al., 2019; Wüstefeld and Bokelmann, 2007). Unlike the RC method, the SC method is dependent on the estimated initial polarisation. The quality of results from the SC method is therefore particularly sensitive to any misalignment of the station orientation and/or miscalculation of the back-azimuth (Eakin et al., 2018). For these reasons, and unless otherwise specified, the results presented in the following sections are from the RC method.

Quality control procedures followed our previous work (Eakin et al., 2021, 2019, 2015) including visual inspection of all waveforms and strict quantitative and qualitative criteria. Further details of the criteria used to determine whether a split (or null) measurement was of acceptable quality are provided in the supplementary text. As an initial step, waveforms were filtered between 0.04-0.125 Hz using a Butterworth bandpass filter. Any event with a signal-to-noise ratio (SNR) of less than 5 for the *SKS*/*PKS* phase was discarded. Using this initially curated dataset, a station misalignment value was estimated. This estimate follows similar investigations by Eakin et al., (2018), that measured the difference between the initial polarisation of *SKS*/*PKS* phase (as determined from the orientation of the uncorrected particle motion) and the source-receiver backazimuth. If the station is found to be misaligned with north then the appropriate orientation correction is applied to all waveforms before further analysis. Station misalignment values applied in this study are available in Table S1.

To help identify regional variations in shear-wave splitting patterns, a stacked result was calculated for each station that had multiple measurements. This was estimated by stacking of the RC error-matrices from all individual split measurements. The station average Φ and δt values are then found from the global minimum of the stacked error surface (Wolfe and Silver, 1998). A further check is performed between the stacked δt result and the mean δt from the individual measurements with a ratio of <1.75 required. This ensures that the stacked

splitting results presented in the final dataset are consistent with the average properties of the individual measurements.

3.3 Mantle flow modelling

We build on the models developed by Davies et al., (2019) to generate a synthetic mantle flow field for comparison with seismic anisotropy observations. Although we focus on the Australian region, our model is global. We solve the equations governing incompressible mantle convection inside a spherical shell, using Fluidity (Davies et al., 2011; Kramer et al., 2012). In our simulation, the inner radius corresponds to the Core Mantle Boundary (CMB) and the outer radius to Earth's surface. Free-slip mechanical boundary conditions are specified at the CMB, with present-day plate kinematics from Müller et al., (2016) prescribed at the surface. Our mesh is generated by refining an icosahedron, resulting in a lateral resolution of 50 km at the surface. This mesh is extruded in the radial direction, with radial spacing increasing linearly from 10 km at the surface to 100 km at the CMB.

We determine the present-day density and temperature fields by adopting a robust thermodynamic approach for converting between seismic and physical structure. This approach, described in Ghelichkhan et al., (2021), uses the upper mantle tomography model of de Laat et al., (2023) above 300 km depth, transitioning smoothly to the whole mantle shear-wave tomography model of S40RTS (Ritsema et al., 2011) for depths below. The former provides higher resolution on lithospheric structure owing to the sensitivity of surface waves. We use Perple_X (Connolly, 2009) alongside the thermodynamic database of Stixrude and Lithgow-Bertelloni (2011) to determine equilibrium phase assemblages throughout the mantle as a function of temperature, and pressure, and their associated anharmonic V_S and density values for pyrolytic mantle. To account for anelastic effects, anharmonic V_S is corrected using an updated version of the Q_5 model by Cammarano et al., (2003). We employ a temperature- and depth-dependent viscosity field, with parameters that are identical to those of Davies et al. (2023), constructed to be compatible with observations of Earth's geoid, heat flux, post-glacial rebound, and CMB ellipticity.

4 SKS & PKS splitting results

Overall, our splitting analysis yielded 1207 measurements across 157 stations, all of which

were individually and visually inspected. A full list is provided in Supporting Information Table S1 in the supporting information. While a single measurement by itself can be unreliable, 67 stations had multiple non-null measurements that produced a stacked splitting result (Figure 3). By utilizing this smaller curated dataset, we focus our attention on those stations with the most robust results. In general, the pattern of individual measurements across all the stations in the study area agrees well with the pattern retrieved from these stacked station results (Figure S2).

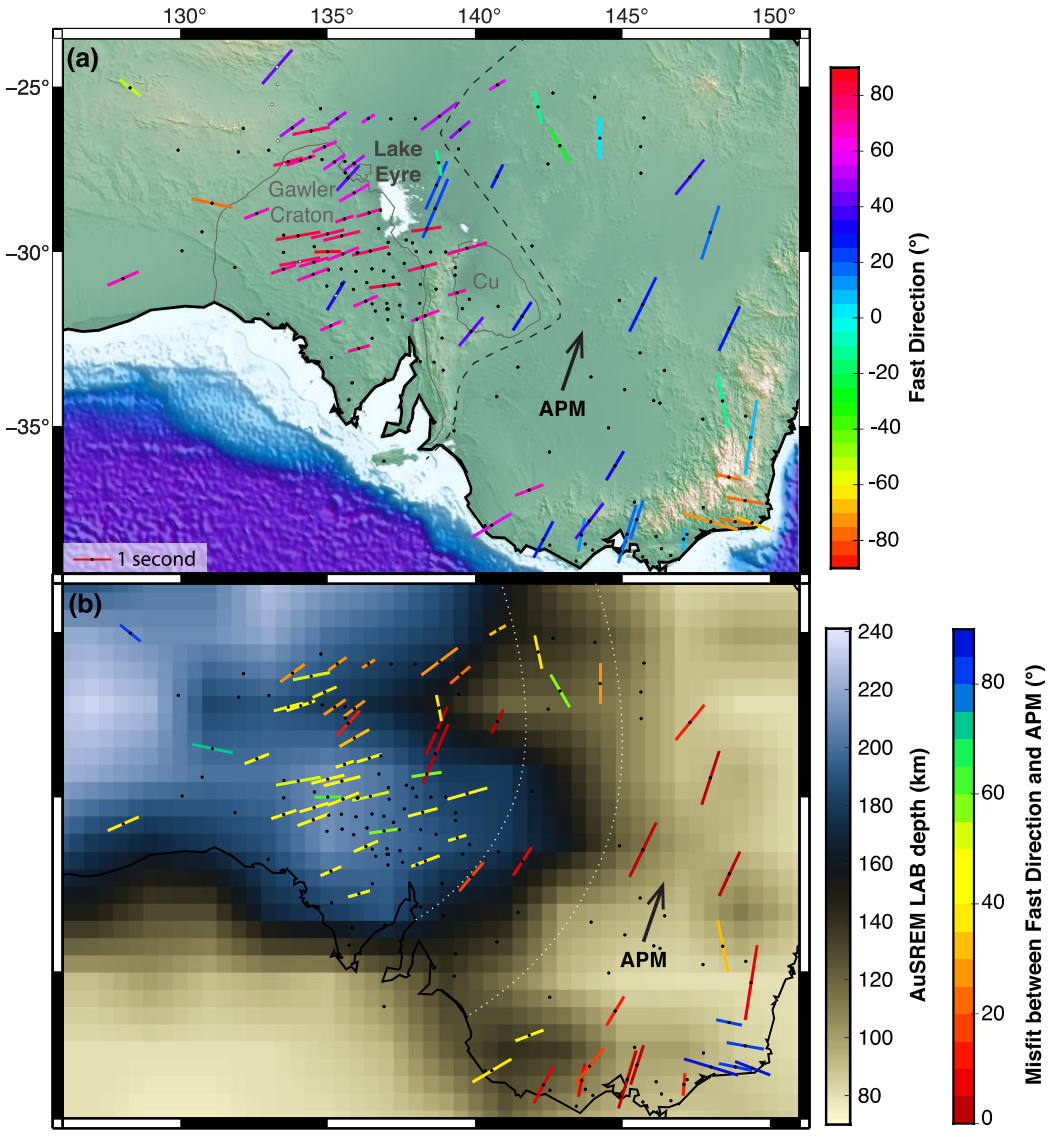

Figure 3. Stacked **KS* splitting results for stations across the study region plotted against (a) surface elevation, and (b) an estimate of lithospheric thickness from AuSREM (Kennett et al., 2012). The stacked splitting parameters for each station are represented by coloured bars,

orientated according to the fast direction, and scaled in length by the delay time. In (a) the bars are coloured according to the fast direction, as indicated by the corresponding colour bar. In (b) colours represent the misfit between the fast direction and the absolute plate motion (APM).

Considering the map of stacked split results in Figure 3a, a broad similarity of splitting parameters can be seen between neighbouring stations indicating a spatially coherent source of seismic anisotropy below. Throughout the Gawler and South Australian Craton there exists a strikingly consistent ENE-WSW splitting pattern (pink/red bars in Figure 3a). The average fast direction (Φ) for the 22 stations within the Gawler Craton is 70°, and 0.80 seconds for the delay time (δt). This is in agreement with our previous study of permanent station MULG (Φ: 79°, δt: 1.1 s) located within the Gawler Craton (Eakin et al., 2021). Other recent studies have reported a similar NE-SW to ENE-WSW trend over the South Australian Craton (Ba et al., 2023; Birkey and Ford, 2022). The spatial extent of this shear-wave splitting pattern, throughout the Gawler Craton and extending eastwards into the Curnamona Province, can now however be seen more clearly. Beyond the craton margins the pattern changes slightly. To the craton's northwest there are only a handful of stations, but these show a change to WNW-ESE fast directions (yellow/orange bars Figure 3a). To the north of the Gawler Craton, over the Lake Eyre region, the fast direction rotates slightly to become more north-easterly (purple coloured bars Figure 3a).

The most notable change is seen crossing from western cratonic Australia into eastern Phanerozoic Australia. The majority of stations in eastern Australia display larger delay times (mean δt: 1.26 s) and N-S to NNE-SSW fast directions (mean Φ: 20°) represented by blue coloured bars in Figure 3a. This orientation is very similar to the absolute plate motion (APM) of the Australian plate, ~6 cm/year at 21° (clockwise from North) in this location, as indicated by the black arrow in Figure 3. Hints of such a correspondence between the fast direction and the absolute plate motion for eastern Phanerozoic Australia have been previously noted based on more limited results (Ba et al., 2023; Bello et al., 2019; Birkey and Ford, 2022). The results of our analysis confirm a similarity between the splitting fast direction and the absolute plate motion for southeastern Australia that is spatially distinct from the pattern over cratonic Australia.

Interestingly, there is a small cluster of five stations in the very south-eastern corner of Australia (~ latitude: 37°S, longitude: 148°E) that show a contrasting but consistent ESE-WNW orientation (ave Φ: -76°, δt: 1.0 s) as indicated by the cluster of orange bars in Figure 3a. Some of these same stations have been previously analysed in other studies: results from Ba et al., (2023) indicated a similar pattern for this sub-group of stations, however the pattern from Bello et al., (2019) was less spatially consistent.

4.1 Comparison with lithospheric thickness

Across the study region, lithospheric thickness reduces drastically from west to east (Figure 1b). Beneath the Gawler and South Australian Craton, where the splitting fast directions are consistently ENE-WSW the lithosphere is ~ 200 km thick (Figure 3b). Over eastern Phanerozoic Australia, where stations show a strong similarity between the fast direction and absolute plate motion (indicated by red bars in Figure 3b), the lithosphere is much thinner with a typical LAB depth ~70-100 km.

A direct comparison of the splitting parameters against LAB depth is plotted in Figure 4 to better quantify this observation. Across the study region we find that the average delay time decreases as the LAB deepens (Figure 4a). This varies from δt >1.0 seconds when the LAB is shallower than 125 km, to an average delay time of ~ 0.8 seconds when the LAB depth is > 175 km. Correspondingly the misfit between absolute plate motion and the fast splitting direction is <20° for most stations located where the LAB depth is <125 km (Figure 4b). The cluster of blue points in Figure 4b that defy this relationship correspond to the anomalous cluster previously identified in the southeastern corner of Australia (i.e. blue bars Figure 3b). For LAB depths greater than 150 km, the misfit between the splitting fast direction and absolute plate motion tends to grow as the lithosphere gets thicker.

There are a small handful of stations with stacked splitting results that fall along the edge of the thick cratonic lithosphere as it transitions to thinner lithosphere. These stations tend to show fast directions that are approximately parallel to the general geometry of the lithospheric step, such as those that fall within the white-dotted band in Figure 3b.

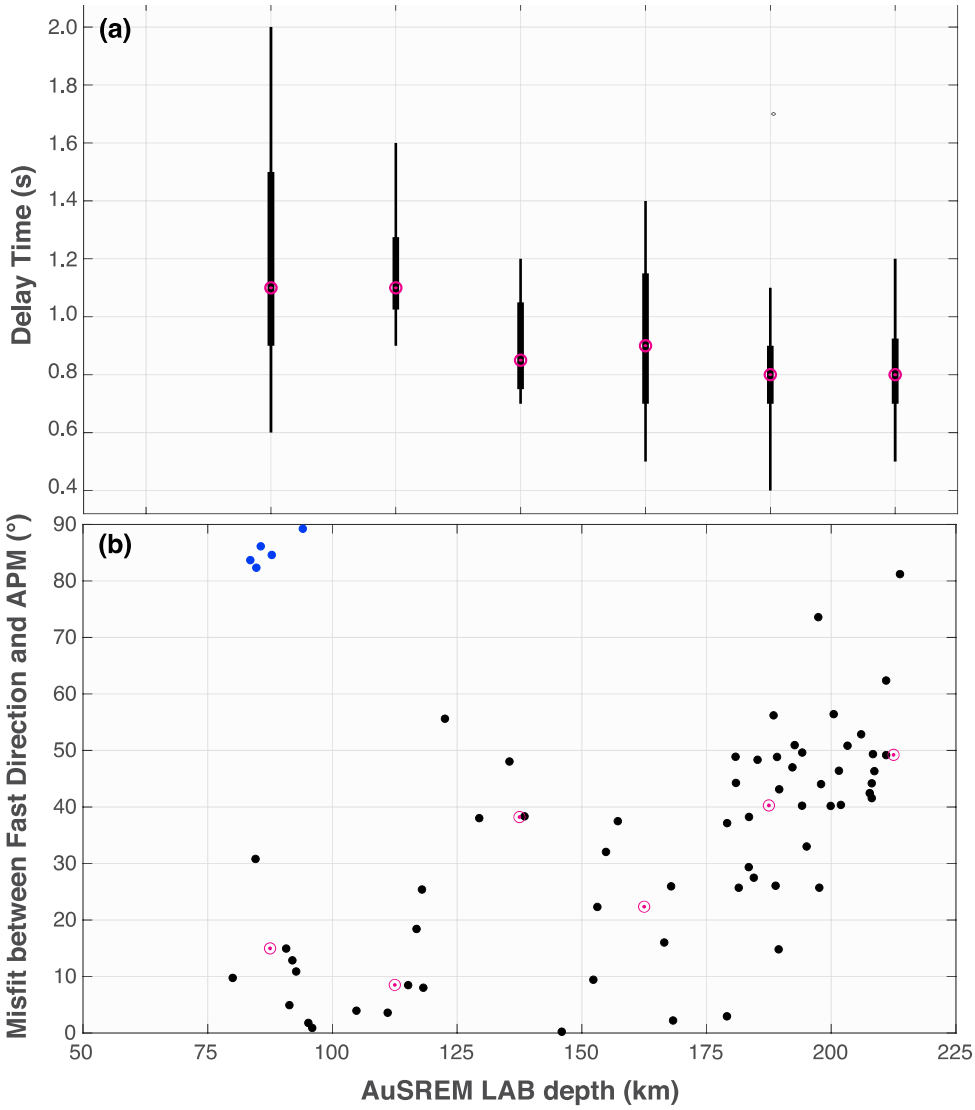

Figure 4. Graph illustrating the relationship between splitting parameters and lithospheric thickness, using the data illustrated in Figure 3b. Median values for each bin are indicated by pink circles. The 5 blue dots in (b) correspond to the cluster of stations in southeast Australia in Figure 3b where results were plotted in the same shade of blue.

4.2 Comparison with the predicted mantle flow field

Uppermost mantle structure and lithospheric thickness variations beneath Australia will influence the underlying asthenospheric flow regime. Geodynamical models that incorporate such upper mantle structure can provide insights on what dynamic processes may be occurring, helping to inform shear-wave splitting observations. In Figure 5 our splitting observations are compared

368 to predictions across the region from a mantle flow simulation (as outlined in Section 3.3). Where
369 the inferred upper mantle viscosity is high at 200 km depth (indicative of the lithosphere), the
370 predicted flow field (small black arrows in Figure 5) generally aligns with absolute plate motion,
371 as prescribed at the surface, demonstrating rigid plate motion within the high viscosity lid. The
372 observed ENE-WSW orientated splitting pattern over this region of high viscosity is therefore
373 inconsistent with the present-day mantle flow direction predicted in our simulation.

374

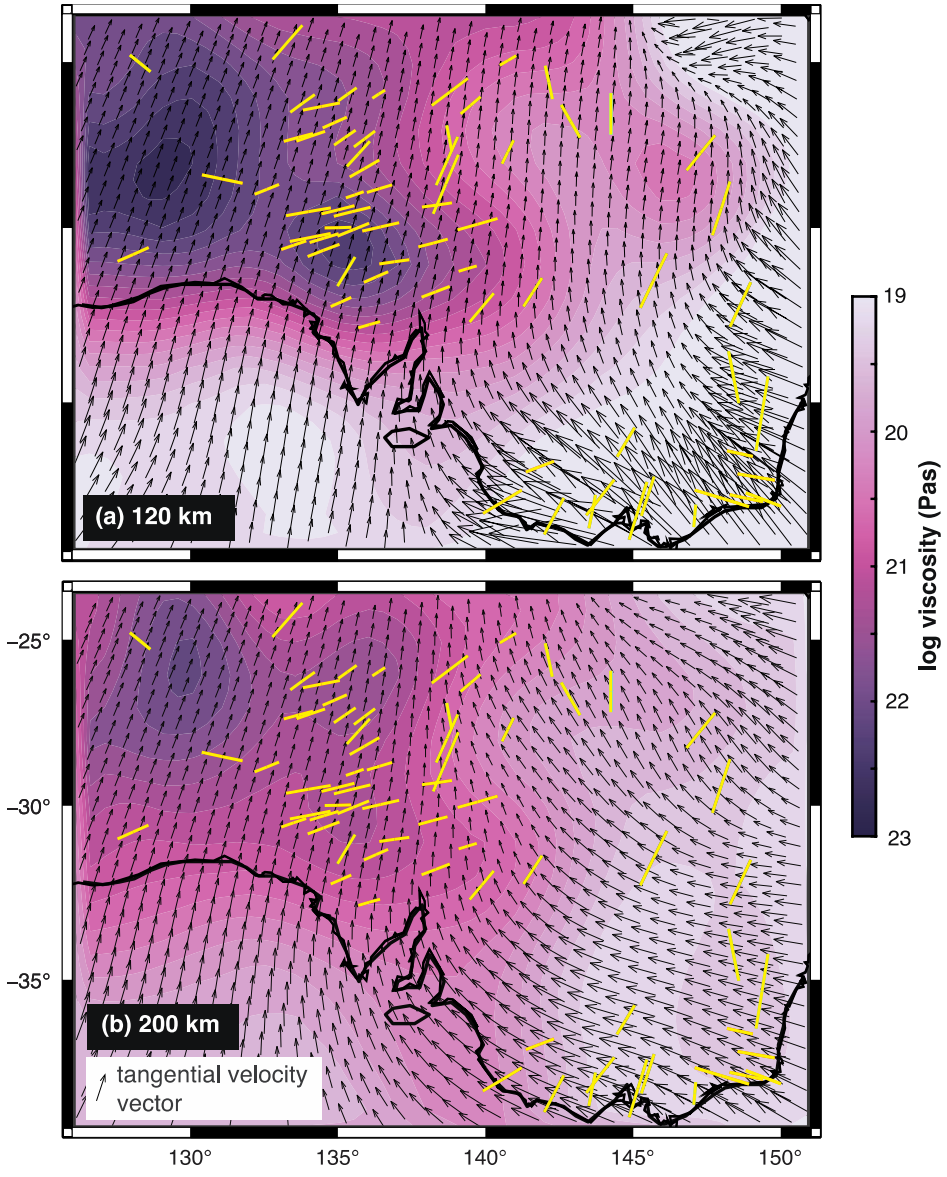

375

376 **Figure 5.** Results of mantle flow simulations at (a) 120 km, and (b) 200 km depth. Stacked **KS*
377 splitting results (same as Figure 3) are plotted in yellow and compared to mantle viscosity and

flow vectors (tangential velocities indicated by small black arrows). Further details for the mantle flow simulation are provided in section 3.3, as well as plots of viscosity and radial velocity at various upper mantle depths in Figure S5.

At the same depth, beneath eastern Australia, the mantle viscosity is predicted to be lower (Figure 5), reflecting the presence of thinner lithosphere and shallower asthenospheric material. In this region the predicted mantle flow-field has a greater E-W component, with mantle material from the east being drawn in towards high-viscosity thick lithosphere in the west and rotating to align with plate motion upon interaction with lithospheric structure. In the simulation, as the Australian continent moves rapidly northwards, the motion of the cratonic lithosphere through the upper mantle creates a region of lower pressure, with lower viscosity asthenospheric material from surrounding areas drawn towards this region. This westwardly flow is strongest in the model in the south-east corner of the study region, matching well (particularly at 200 km depth, Fig. 5b) with the sub-group of 5 stations that showed anomalous ESE-WNW orientated splitting (orange bars in Fig. 3a). In general, however, the shear-wave splitting pattern over eastern Australia shows a greater similarity to the absolute plate motion, rather than the asthenospheric flow-field predicted in the mantle flow simulation.

5 Discussion

Our results demonstrate clear and spatially coherent shear-wave splitting patterns (Figures 3-4). This splitting pattern appears to morph from an ENE-WSW alignment over the thicker lithosphere of the South Australian Craton, to a NNE-SSW alignment, that follows the APM for stations located above the thinner Phanerozoic lithosphere in the east. This clear pattern is in contrast to the weak splitting and complex anisotropy often inferred by the earliest studies of *SKS* splitting in Australia (e.g. Clitheroe and van der Hilst, 1998). Further context regarding the emergence of coherent seismic anisotropy beneath Australia can be found in the supplementary text (section ST2). As is common practice for **KS* splitting studies at the continental scale (e.g. Ba et al., 2023; Eakin et al., 2010), we have presented stacked splitting results at each station. Such stacked results allow for interpretation in terms of a single (and relatively simple) layer of anisotropy. Analysis of the back-azimuthal variations lends support to such a single-layer interpretation (Figures S9-S10), and we find that complex or multi-layered anisotropy is not

408 required to explain the results (refer to section ST3 of the supplementary text for extended details).

409 5.1 Anisotropic Contributions from the Lithosphere versus Asthenosphere

410 Placing the results into the context of simple (i.e. single-layer) anisotropy allows for a
411 straightforward interpretation, that is consistent with geological constraints. The relationship
412 between lithospheric thickness and alignment of the fast direction with the absolute plate motion
413 (Figures 3-4) can be easily explained. Where the lithosphere is relatively young and thin (<100 km
414 thick) over eastern Phanerozoic Australia (Figure 3) the contribution from lithospheric anisotropic
415 fabrics is likely small. Instead, the anisotropic signal from the asthenosphere can dominate,
416 resulting in splitting fast directions that match with the absolute plate motion (Figure 3). This
417 suggests shear of the underlying mantle asthenosphere by the fast plate motion above, as has long
418 been proposed by surface wave studies that imaged strong APM aligned azimuthal anisotropy at
419 the base of the plate (e.g. Debayle et al., 2005).

420 Conversely where the lithosphere is relatively old and thick (>175 km thick) over cratonic
421 Precambrian Australia (Figure 3), the consistent ENE-WSW orientations suggests that anisotropic
422 contributions from fossilized lithospheric fabrics dominate the shear-wave splitting signal. This is
423 not to say that strong shear of the asthenosphere below is no longer occurring (as has been imaged
424 by surface waves), but that the shear-wave splitting appears most sensitive to shallower
425 lithospheric anisotropy in the mantle's uppermost 200 km. Such an observation is supported by
426 previous modelling of vertically varying anisotropy and synthetic seismograms by Saltzer et al.,
427 (2000). Their work suggested that **KS* splitting measurements may be more biased towards the
428 upper portion of the anisotropic medium with the greatest sensitivity at around one-third of the
429 depth of the total extent of the anisotropy. They suggest that this explains why many stable
430 continents display fast splitting directions that mirror surface geology (e.g. Silver, 1996), which is
431 also the case here (Figure 6).

432 The reduced delay times (< 1 second) for stations situated on-top of thick lithosphere
433 (Figure 4a) however would suggest that when the primary source of anisotropy is from the
434 lithosphere, this is not as strong as when the lithosphere is thin (< 125 km) and the primary source
435 is more likely from asthenospheric flow. Alternatively, when the lithosphere is thick and
436 lithospheric contributions dominate, a more minor but opposing contribution from the deeper
437 asthenosphere could cause a slight reduction of the delay times.

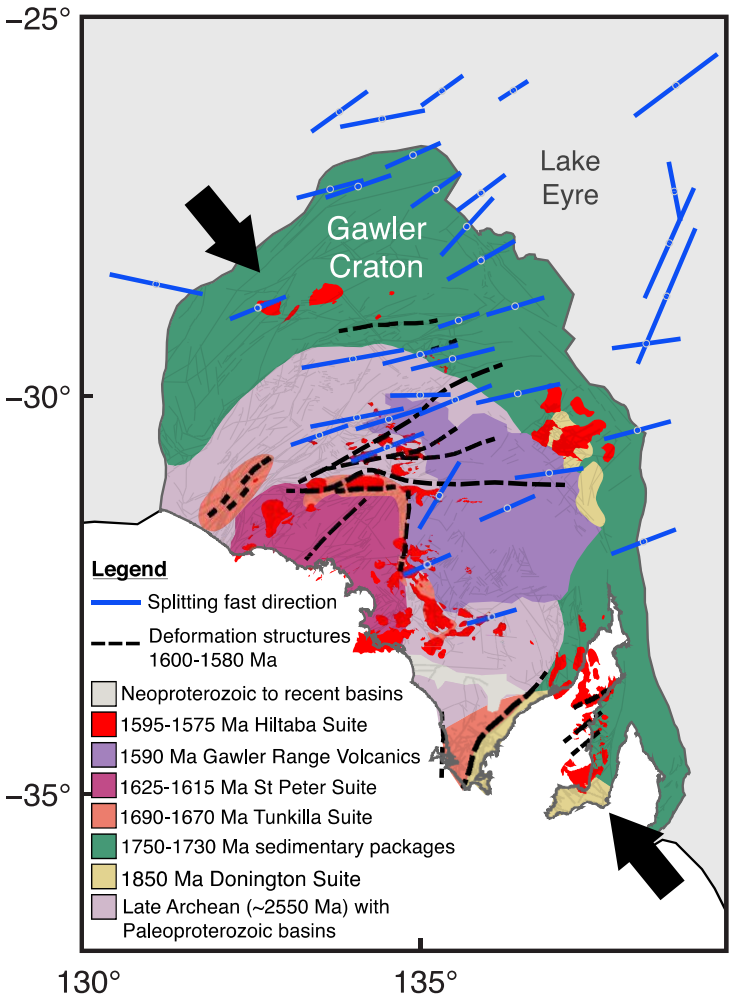

Figure 6. Comparison of stacked **KS* splitting results (blue bars) with a simplified geological map of the Gawler Craton, modified from Hand et al., (2007). Location of crustal deformation structures are shown (thick dashed black lines) that either formed or reactivated during NW-SE directed compression (as indicated by the large black arrows) during the interval 1600-1580 Ma. The similar pattern of Archean-Early Mesoproterozoic faults (thin grey lines), as well as coeval volcanism from the Hiltaba Suite (red polygons), are overlain from Cowley, (2006).

Considering that the splitting pattern changes drastically from west to east across the study area, the most plausible explanation appears to be a change in the primary source of anisotropy from lithospheric to asthenospheric. In Australia, studies of azimuthal anisotropy from surface waves also tend to show clear east-west trending fast axes at lithospheric depths (~ 50-150 km) within the South Australian Craton (e.g. Fishwick et al., 2008; Simons et al., 2002). Moving

eastwards as the lithosphere thins, these fast axes tend to change orientation within the same depth slice (e.g. Figure S7), but it is difficult for surface waves to delineate lateral contrasts in seismic anisotropy. In contrast, Quasi-Love wave scatterers, which are sensitive to lateral gradients in seismic anisotropy at upper mantle depths (~100-200 km) (Eakin, 2021), can often be traced to the edge of thick lithosphere and to locations where a change in our shear-wave splitting pattern occurs (Figure S6).

5.2 Implications for the South Australian Craton

Over the South Australian Craton, which encompasses the Archean-Proterozoic Gawler Craton and Curnamona Province, the **KS* splitting displays a consistent ENE-WSW orientated pattern (Figure 3a). North of our study area, the orientation of the fast direction has previously been shown to flip to match the NW-SE aligned terrane boundaries within the North Australia Craton (Eakin et al., 2021). This likely indicates that the lithospheric anisotropic fabric differs between the two major cratonic domains, reflecting different tectonic histories.

Within the South Australia Craton, upon first impressions, the ENE-WSW orientation of the anisotropy does not appear to match the outline of the major geological provinces or crustal boundaries (Figure S8), as noted by Birkey and Ford (2022). However, upon closer inspection, the ENE-WSW orientated fast directions agree very well with the structural trends found internally within the Gawler Craton, which are preserved as a series of E-W to NE-SW trending faults (Figure 6). Several of these major crustal shear zones and deformation structures (highlighted by thick black dashed lines in Figure 6) either formed or were reactivated during the mid-Proterozoic around 1.6 to 1.58 billion years ago (Hand et al., 2007). This time period is associated with the last major deformational event that impacted the entire Gawler Craton, due to large-scale NW-SE directed compression (indicated by the thick black arrows in Figure 6) (Hand et al., 2007). Such a tectonic history is consistent with the anisotropic geometry retrieved by this study. This strongly suggests that the splitting pattern over the Gawler Craton (and surroundings) is a manifestation of fossilised LPO fabrics frozen into the lithosphere and preserved for well over a billion years. The consistency of splitting pattern over such a large area suggests widespread uniform deformation of the lithosphere during the Proterozoic, before it fully cratonized.

Intriguingly at the time of deformation, the region also experienced significant volcanism and heating, as recorded by the emplacement of the Gawler Range Volcanics (~1590 Ma) and the

Hiltaba Suite (1595-1575 Ma). Both magmatic events impacted large swaths of the Gawler Craton, as indicated in Figure 6. The introduction of heat and melts from this volcanism may have substantially weakened the lithosphere and further aided widespread deformation, producing the significant lithospheric LPO fabrics still seen today. After the emplacement of the Hiltaba Suite, volcanism ceased in the region, allowing the lithosphere to cool, strengthen, and preserve the anisotropy over the following 1.6 billion years.

5.3 Deviations of the asthenospheric flow associated with LAB topography

While there appears a clear relationship between the splitting parameters and lithospheric thickness (Figure 4), there are some locations where the splitting fast directions neither follow the APM-aligned mantle flow direction nor the inferred orientation of the lithospheric fabric. One such location is along the eastern edge of the thick cratonic lithosphere (highlighted by the dotted white band in Figure 3b). While there are only a small number of stations in this zone, intriguingly the orientation of the fast direction appears to follow the general trend of the lithospheric step, as indicated by the AuSREM LAB model. This perhaps hints at a deviation of the mantle flow field around the edge of the cratonic root. Such a mechanism can be seen in our mantle flow simulations, particularly at 120 km depth along the north-eastern boundary of the higher viscosity region (Figure 5a). However, this location varies with depth in the simulations and is offset further east compared to the lithospheric step suggested by the AuSREM LAB model (Figure 3b). Deviations of flow around the continental keel have been invoked previously to explain departures of the splitting fast direction from the absolute plate motion of Australia (Ba et al., 2023; Bello et al., 2019; Clitheroe and van der Hilst, 1998; Heintz and Kennett, 2005). However, it has not previously been imaged parallel to, and directly in the vicinity of, the lithospheric step as seen in Figure 3b. Alternatively, some of the stations within this band, particularly in the north, match well with the predicted upper mantle flow from our simulation (Figure 5). This suggests that the pattern could also be reproduced by mantle flow drawn in towards the fast-moving continent, rather than flow diverted around the lithospheric step.

Another interesting location where the splitting fast direction departs from the general trend of APM alignment is the cluster of results in the southeast corner of the study area, highlighted in blue in Figures 3b and 4. In this region the lithosphere is quite thin (< 100 km), so a substantial contribution from lithospheric fabrics would not be expected. Intriguingly, however, the splitting

pattern in this location matches well with the westward directed mantle flow predicted by our geodynamic simulation along eastern Australia, especially at ~200 km depth (Figure 5b). This may suggest that it is the result of a similar process, whereby asthenospheric material from beneath the Tasman Sea is being drawn in towards the higher viscosity lithospheric keel of the Australian continent. Why the process would be localized to just this area remains unclear, but perhaps suggests more complex lithospheric architecture in this region than is presently resolved by tomographic models, such as that by de Laat et al., (2023) utilized here.

To the south of this E-W orientated splitting cluster lies a well imaged low velocity anomaly in the shallow upper mantle of the Bass Strait (e.g. de Laat et al., 2023). This low velocity feature has been variously attributed to localized edge-driven convection (Davies and Rawlinson, 2014; Rawlinson et al., 2017), and/or a mantle plume (Davies et al., 2015), both of which would induce small-scale deviations of the mantle flow-field. Additionally, strong scattering of Love-to-Rayleigh waves beneath the Bass Strait have been observed (Eakin, 2021), indicative of lateral gradients in upper mantle anisotropy. Together these observations and models suggest small-scale convective processes are likely occurring beneath the Bass Strait that may influence the anomalous patterns of seismic anisotropy beneath southeastern Australia.

6 Conclusion

From analyzing **KS* splitting at over 170 stations and focusing on those that could provide high-quality stacked results, coherent but regionally variable anisotropic patterns have emerged beneath south and eastern Australia. In regions of comparatively thin lithosphere (70-125 km), we find fast directions aligned with Australia's rapid plate motion, as predicted from surface wave studies. This demonstrates that lithospheric contributions are minimised beneath eastern Australia, with splitting patterns principally governed by asthenospheric flow. Conversely, where the lithosphere is thicker beneath the South Australian Craton, ancient deformational fabrics appear to dominate that have likely been preserved within the lithospheric mantle. The trend of this anisotropic fabric is comparable with deformational structures from the Early-Mesoproterozoic found within the Gawler Craton. Such findings imply widespread and uniform deformation of the region, coeval with the addition of heat and the emplacement of the Hiltaba Suite and Gawler Range Volcanics, before the South Australian lithosphere cratonized at ~1.6-1.5 Ga.

Lithospheric thickness variations therefore appear to exert a first-order control on the

anisotropic signal retrieved from shear-wave splitting beneath Australia. While continental scale imaging of the LAB beneath Australia has been achieved by seismic tomography (e.g. Kennett and Salmon, 2012), it is more difficult to resolve sharp lateral contrasts in lithospheric age and thickness that may demarcate important tectonic boundaries such as the enigmatic Tasman Line. With the ongoing expansion of seismic data collection across Australia, further detailed investigations of the anisotropic structure may therefore hold significant potential for unveiling the expansive tectonic history and lithospheric architecture of this ancient continent.

Acknowledgments

We acknowledge the traditional custodians on whose land seismic stations were deployed. SA and CME were supported by Australian Research Council grant DE190100062. The Lake Eyre Basin seismic array, any many of the previous temporary deployments, were made possible by funding from AuScope (https://auscope.org.au), instrumentation from the Australian National Seismic Imaging Resource (ANSIR), and contributions from staff at the Research School of Earth Sciences of the Australian National University, most notably Robert Pickle and Michelle Salmon. The AusArray-SA deployment was supported by the Geological Survey of South Australia (GSSA), with instrumentation from ANSIR and Geoscience Australia. The GSSA thanks Isaac Axford, Goran Boren, Ann Goleby, Liz Jagodzinski, Christine Selway, Kate Selway, John Stephenson, Judy and Ed Zajer, Michelle Salmon, Robert Pickle, and Colin Telfer for their invaluable contributions to AusArray-SA. We are incredibly grateful to landholders, traditional owners, and the Department of Defence for granting land access for the seismic arrays. JPOD publishes with the permission of the Director of the Geological Survey of South Australia.

We thank Janneke de Laat for sharing the *Aus22* shear-wave velocity model prior to its subsequent publication (de Laat et al., 2023). Our geodynamical simulations were supported by the Australian Government's National Collaborative Research Infrastructure Strategy (NCRIS), with access to computational resources provided on Gadi through the National Computational Merit Allocation Scheme and the ANU Merit Allocation Scheme.

Open Research

A table of all shear wave splitting measurements made during this study can be found in the supporting information (Table S1), and will be available from the ANU Data Commons

repository (https://datacommons.anu.edu.au/; doi to be provided upon acceptance). Splitting measurements were processed using SplitLab version 1.2 updated by Robert Porritt (https://robporritt.wordpress.com/software/). Figures were made with the aid of Generic Mapping tools (Wessel et al., 2013), scientific color maps from (Crameri et al., 2020), and geological maps available via the South Australia Resources Information Gateway (SARIG, https://map.sarig.sa.gov.au/).

Seismic data from the Lake Eyre Basin (5G, 10.7914/SN/5G_2018, Eakin, 2018) and AusArray-SA (6K, 10.7914/SN/6K_2020, O'Donnell et al., 2020) is deposited with the Australian Passive Seismic Server (AusPass; http://auspass.edu.au/) hosted at the Research School of Earth Sciences, Australian National University, and will be publicly available from June 2024. Waveforms and meta-data from the ensuing list (network name, network code, DOI) of contributing permanent and temporary seismic networks were accessed through AusPass and/or the Incorporated Research Institutions for Seismology Data Management Center (IRIS DMC; https://ds.iris.edu/ds/nodes/dmc): ANSN, AU, 10.26186/144675; AUSIS, S1, 10.7914/SN/S1; SQSPA, 1E, 10.7914/SN/1E_2013; BASS, 1P, 10.7914/SN/1P_2011; AQT, 1Q, 10.7914/SN/1Q_2016; MAL, 3G, 10.7914/SN/3G_2018; Lake Eyre, 5G, 10.7914/SN/5G_2018; ASR, 5J, 10.7914/SN/5J_2017; BILBY, 6F, 10.7914/SN/6F_2008; AusArray-SA, 6K, 10.7914/SN/6K_2020; TIGGER BB, 7H, 10.7914/SN/7H_2001; TASMAL, 7I, 10.7914/SN/7I_2003; SOC, 7K, 10.7914/SN/7K_2007.

References

Agrawal, S., Eakin, C.M., O'donnell, J., 2022. Characterizing the cover across South Australia: a simple passive-seismic method for estimating sedimentary thickness. Geophys. J. Int. 231, 1850–1864. https://doi.org/10.1093/GJI/GGAC294

Ba, K., Gao, S.S., Song, J., Liu, K.H., 2023. Seismic Azimuthal Anisotropy Beneath a Fast Moving Ancient Continent: Constraints From Shear Wave Splitting Analysis in Australia. J. Geophys. Res. Solid Earth 128. https://doi.org/10.1029/2022JB025866

Ball, P.W., Czarnota, K., White, N.J., Klöcking, M., Davies, D.R., 2021. Thermal Structure of Eastern Australia's Upper Mantle and Its Relationship to Cenozoic Volcanic Activity and Dynamic Topography. Geochemistry, Geophys. Geosystems 22, e2021GC009717. https://doi.org/10.1029/2021GC009717

Bello, M., Cornwell, D.G., Rawlinson, N., Reading, A.M., 2019. Insights into the structure and dynamics of the upper mantle beneath Bass Strait, southeast Australia, using shear wave splitting. Phys. Earth Planet. Inter. 289, 45–62. https://doi.org/10.1016/J.PEPI.2019.02.002

Betts, P.G., Giles, D., 2006. The 1800-1100 Ma tectonic evolution of Australia. Precambrian Res. 144, 92–125. https://doi.org/10.1016/j.precamres.2005.11.006

Bezada, M.J., Smale, J., 2019. Lateral Variations in Lithospheric Mantle Structure Control the Location of Intracontinental Seismicity in Australia. Geophys. Res. Lett. 46, 12862–12869. https://doi.org/10.1029/2019GL084848

Birkey, A., Ford, H.A., 2022. Anisotropic Structure of the Australian Continent. Front. Earth Sci. 10, 2528. https://doi.org/10.3389/FEART.2022.1055480

Bowman, J.R., Ando, M., 1987. Shear-wave splitting in the upper-mantle wedge above the Tonga subduction zone. Geophys. J. Int. 88, 25–41. https://doi.org/10.1111/j.1365-246X.1987.tb01367.x

Cammarano, F., Goes, S., Vacher, P., Giardini, D., 2003. Inferring upper-mantle temperatures from seismic velocities. Phys. Earth Planet. Inter. 138, 197–222. https://doi.org/10.1016/S0031-9201(03)00156-0

Chen, X., Levin, V., Yuan, H., 2021. Small Shear Wave Splitting Delays Suggest Weak

Anisotropy in Cratonic Mantle Lithosphere. Geophys. Res. Lett. e2021GL093861. https://doi.org/10.1029/2021GL093861

Clitheroe, G., van der Hilst, R., 1998. Complex Anisotropy in the Australian Lithosphere from Shear-wave Splitting in Broad-band SKS Records. Geodyn. Ser. 26, 73–78. https://doi.org/10.1002/9781118670095.ch5

Connolly, J.A.D., 2009. The geodynamic equation of state: What and how. Geochemistry, Geophys. Geosystems 10, 10014. https://doi.org/10.1029/2009GC002540

Cowley, W.M., 2006. Solid geology of South Australia: peeling away the cover. MESA J. 43, 4–15.

Crameri, F., Shephard, G.E., Heron, P.J., 2020. The misuse of colour in science communication. Nat. Commun. 11, 5444. https://doi.org/10.1038/s41467-020-19160-7

Davies, D.R., Ghelichkhan, S., Hoggard, M.J., Valentine, A.P., Richards, F.D., 2023. Observations and Models of Dynamic Topography: Current Status and Future Directions, in: Duarte, J.C. (Ed.), Dynamics of Plate Tectonics and Mantle Convection. Elsevier, pp. 223–269. https://doi.org/10.1016/B978-0-323-85733-8.00017-2

Davies, D.R., Rawlinson, N., 2014. On the origin of recent intraplate volcanism in Australia. Geology 42, 1031–1034. https://doi.org/10.1130/G36093.1

Davies, D.R., Rawlinson, N., Iaffaldano, G., Campbell, I.H., 2015. Lithospheric controls on magma composition along Earth's longest continental hotspot track. Nature 525, 511–514. https://doi.org/10.1038/nature14903

Davies, D.R., Valentine, A.P., Kramer, S.C., Rawlinson, N., Hoggard, M.J., Eakin, C.M., Wilson, C.R., 2019. Earth's multi-scale topographic response to global mantle flow. Nat. Geosci. 12. https://doi.org/10.1038/s41561-019-0441-4

Davies, D.R., Wilson, C.R., Kramer, S.C., 2011. Fluidity: A fully unstructured anisotropic adaptive mesh computational modeling framework for geodynamics. Geochemistry, Geophys. Geosystems 12. https://doi.org/10.1029/2011GC003551

de Laat, J.I., Lebedev, S., Celli, N.L., Bonadio, R., Chagas de Melo, B., Rawlinson, N., 2023. Structure and evolution of the Australian plate and underlying upper mantle from waveform

tomography with massive data sets. Geophys. J. Int. 234, 153–189. https://doi.org/10.1093/GJI/GGAD062

Debayle, E., Kennett, B., Priestley, K., 2005. Global azimuthal seismic anisotropy and the unique plate-motion deformation of Australia. Nature 433, 509–512. https://doi.org/10.1038/nature03247

Debayle, E., Ricard, Y., 2013. Seismic observations of large-scale deformation at the bottom of fast-moving plates. Earth Planet. Sci. Lett. 376, 165–177. https://doi.org/10.1016/j.epsl.2013.06.025

Direen, N.G., Crawford, A.J., 2003. The Tasman Line: Where is it, what is it, and is it Australia's Rodinian breakup boundary? Aust. J. Earth Sci. 50, 491–502. https://doi.org/10.1046/J.1440-0952.2003.01005.X

Duvernay, T., Davies, D.R., Mathews, C.R., Gibson, A.H., Kramer, S.C., 2021. Linking Intraplate Volcanism to Lithospheric Structure and Asthenospheric Flow. Geochemistry, Geophys. Geosystems 22, e2021GC009953. https://doi.org/10.1029/2021GC009953

Eakin, C., 2019. Seismicity, Minerals, and Craton margins: The Lake Eyre Basin Seismic Deployment. ASEG Ext. Abstr. 1, 1–2. https://doi.org/10.1080/22020586.2019.12072989

Eakin, C., 2018. Lake Eyre Basin [Data set]. https://doi.org/10.7914/SN/5G_2018

Eakin, C.M., 2021. Quasi-Love wave scattering reveals tectonic history of Australia and its margins reflected by mantle anisotropy. Commun. Earth Environ. 2. https://doi.org/10.1038/s43247-021-00276-7

Eakin, C.M., Flashman, C., Agrawal, S., 2021. Seismic anisotropy beneath Central Australia: A record of ancient lithospheric deformation. Tectonophysics 820, 229123. https://doi.org/10.1016/J.TECTO.2021.229123

Eakin, C.M., Long, M.D., Wagner, L.S., Beck, S.L., Tavera, H., 2015. Upper mantle anisotropy beneath Peru from SKS splitting: Constraints on flat slab dynamics and interaction with the Nazca Ridge. Earth Planet. Sci. Lett. 412, 152–162. https://doi.org/10.1016/j.epsl.2014.12.015

Eakin, C.M., Obrebski, M., Allen, R.M., Boyarko, D.C., Brudzinski, M.R., Porritt, R., 2010.

673 Seismic anisotropy beneath Cascadia and the Mendocino triple junction: Interaction of the
674 subducting slab with mantle flow. Earth Planet. Sci. Lett. 297, 627–632.
675 https://doi.org/10.1016/j.epsl.2010.07.015

676 Eakin, C.M., Rychert, C.A., Harmon, N., 2018. The Role of Oceanic Transform Faults in
677 Seafloor Spreading: A Global Perspective From Seismic Anisotropy. J. Geophys. Res. Solid
678 Earth 123, 1736–1751. https://doi.org/10.1002/2017JB015176

679 Eakin, C.M., Wirth, E.A., Wallace, A., Ulberg, C.W., Creager, K.C., Abers, G.A., 2019. SKS
680 Splitting Beneath Mount St. Helens: Constraints on Subslab Mantle Entrainment.
681 Geochemistry, Geophys. Geosystems 20. https://doi.org/10.1029/2019GC008433

682 Farrington, R.J., Stegman, D.R., Moresi, L.N., Sandiford, M., May, D.A., 2010. Interactions of
683 3D mantle flow and continental lithosphere near passive margins. Tectonophysics 483, 20–
684 28. https://doi.org/10.1016/j.tecto.2009.10.008

685 Fichtner, A., Kennett, B.L.N., Igel, H., Bunge, H.P., 2010. Full waveform tomography for
686 radially anisotropic structure: New insights into present and past states of the Australasian
687 upper mantle. Earth Planet. Sci. Lett. 290, 270–280.
688 https://doi.org/10.1016/j.epsl.2009.12.003

689 Fishwick, S., Heintz, M., Kennett, B.L.N., Reading, A.M., Yoshizawa, K., 2008. Steps in
690 lithospheric thickness within eastern Australia, evidence from surface wave tomography.
691 Tectonics 27. https://doi.org/10.1029/2007TC002116

692 Ghelichkhan, S., Bunge, H.P., Oeser, J., 2021. Global mantle flow retrodictions for the early
693 Cenozoic using an adjoint method: evolving dynamic topographies, deep mantle structures,
694 flow trajectories and sublithospheric stresses. Geophys. J. Int. 226, 1432–1460.
695 https://doi.org/10.1093/GJI/GGAB108

696 Glen, R.A., 2005. The Tasmanides of eastern Australia, in: Vaughan, A.P.M., Leat, P.T.,
697 Pankhurst, R.J. (Eds.), Terrane Processes at the Margins of Gondwana. Geological Society
698 of London, Special Publication, London, pp. 23–96.

699 Hand, M., Reid, A., Jagodzinski, L., 2007. Tectonic Framework and Evolution of the Gawler
700 Craton, Southern Australia. Econ. Geol. 102, 1377–1395.

https://doi.org/10.2113/GSECONGEO.102.8.1377

Heintz, M., Kennett, B.L.N., 2006. The apparently isotropic Australian upper mantle. Geophys. Res. Lett. 33, L15319. https://doi.org/10.1029/2006GL026401

Heintz, M., Kennett, B.L.N., 2005. Continental scale shear wave splitting analysis: Investigation of seismic anisotropy underneath the Australian continent. Earth Planet. Sci. Lett. 236, 106–119. https://doi.org/10.1016/j.epsl.2005.05.003

Hoggard, M.J., Czarnota, K., Richards, F.D., Huston, D.L., Jaques, A.L., Ghelichkhan, S., 2020. Global distribution of sediment-hosted metals controlled by craton edge stability. Nat. Geosci. 13, 504–510. https://doi.org/10.1038/s41561-020-0593-2

Karato, S., Jung, H., Katayama, I., Skemer, P., 2008. Geodynamic Significance of Seismic Anisotropy of the Upper Mantle: New Insights from Laboratory Studies. Annu. Rev. Earth Planet. Sci. 36, 59–95. https://doi.org/10.1146/annurev.earth.36.031207.124120

Kennett, B.L.N., Fichtner, A., Fishwick, S., Yoshizawa, K., 2012. Australian Seismological Reference Model (AuSREM): mantle component. Geophys. J. Int. 192, 871–887. https://doi.org/10.1093/gji/ggs065

Kennett, B.L.N., Salmon, M., 2012. AuSREM: Australian Seismological Reference Model. Aust. J. Earth Sci. 59, 1091–1103. https://doi.org/10.1080/08120099.2012.736406

Kramer, S.C., Wilson, C.R., Davies, D.R., 2012. An implicit free surface algorithm for geodynamical simulations. Phys. Earth Planet. Inter. 194–195, 25–37. https://doi.org/10.1016/J.PEPI.2012.01.001

Kreemer, C., Blewitt, G., Klein, E.C., 2014. A geodetic plate motion and Global Strain Rate Model. Geochemistry, Geophys. Geosystems 15, 3849–3889. https://doi.org/10.1002/2014GC005407

Müller, R.D., Seton, M., Zahirovic, S., Williams, S.E., Matthews, K.J., Wright, N.M., Shephard, G.E., Maloney, K.T., Barnett-Moore, N., Hosseinpour, M., Bower, D.J., Cannon, J., 2016. Ocean Basin Evolution and Global-Scale Plate Reorganization Events Since Pangea Breakup. https://doi.org/10.1146/annurev-earth-060115-012211 44, 107–138. https://doi.org/10.1146/ANNUREV-EARTH-060115-012211

729 Myers, J.S., Shaw, R.D., Tyler, I.M., 1996. Tectonic evolution of Proterozoic Australia.
730 TECTONICS 15, 1431–1446. https://doi.org/10.1029/96TC02356

731 Nicolas, A., Christensen, N.I., 1987. Formation of anisotropy in upper mantle peridotites: A
732 review, in: Fuchs, K., Froidevaux, C. (Eds.), Composition, Structure and Dynamics of the
733 Lithosphere-Asthenosphere System. American Geophysical Union, pp. 111–123.
734 https://doi.org/10.1029/GD016p0111

735 O'Donnell, J.P., Thiel, S., Robertson, K., Gorbatov, A., Eakin, C., 2020. Using seismic
736 tomography to inform mineral exploration in South Australia: the AusArray SA broadband
737 seismic array. MESA J. 93, 24–31.

738 O'Donnell, John Paul, Thiel, S., Robertson, K., Gorbatov, A., Goleby, B., 2020. AusArray SA
739 [Data set]. https://doi.org/10.7914/SN/6K_2020

740 Özalaybey, S., Chen, W.P., 1999. Frequency-dependent analysis of SKS/SKKS waveforms
741 observed in Australia: Evidence for null birefringence. Phys. Earth Planet. Inter. 114, 197–
742 210. https://doi.org/10.1016/S0031-9201(99)00058-8

743 Rawlinson, N., Davies, D.R., Pilia, S., 2017. The mechanisms underpinning Cenozoic intraplate
744 volcanism in eastern Australia: Insights from seismic tomography and geodynamic
745 modeling. Geophys. Res. Lett. 44, 9681–9690.
746 https://doi.org/https://doi.org/10.1002/2017GL074911

747 Raymond, O.L., Totterdell, J.M., Woods, M.A., Stewart, A.J., 2018. Australian Geological
748 Provinces 2018.01 edition. https://doi.org/http://pid.geoscience.gov.au/dataset/ga/116823

749 Ritsema, J., Deuss, A., van Heijst, H.J., Woodhouse, J.H., 2011. S40RTS: a degree-40 shear-
750 velocity model for the mantle from new Rayleigh wave dispersion, teleseismic traveltime
751 and normal-mode splitting function measurements. Geophys. J. Int. 184, 1223–1236.
752 https://doi.org/10.1111/j.1365-246X.2010.04884.x

753 Saltzer, R.L., Gaherty, J.B., Jordan, T.H., 2000. How are vertical shear wave splitting
754 measurements affected by variations in the orientation of azimuthal anisotropy with depth?
755 Geophys. J. Int. 141, 374–390. https://doi.org/10.1046/j.1365-246x.2000.00088.x

756 Silver, P.G., 1996. SEISMIC ANISOTROPY BENEATH THE CONTINENTS: Probing the

Depths of Geology. Annu. Rev. Earth Planet. Sci. 24, 385–432. https://doi.org/10.1146/annurev.earth.24.1.385

Silver, P.G., Chan, W.W., 1991. Shear Wave Splitting and Sub continental Mantle Deformation. J. Geophys. Res. Solid Earth 96, 16429–16454. https://doi.org/10.1029/91JB00899

Simons, F.J., van der Hilst, R.D., Montagner, J.P., Zielhuis, A., 2002. Multimode Rayleigh wave inversion for heterogeneity and azimuthal anisotropy of the Australian upper mantle. Geophys. J. Int. 151, 738–754. https://doi.org/10.1046/j.1365-246X.2002.01787.x

Stixrude, L., Lithgow-Bertelloni, C., 2011. Thermodynamics of mantle minerals - II. Phase equilibria. Geophys. J. Int. 184, 1180–1213. https://doi.org/10.1111/J.1365-246X.2010.04890.X

Vinnik, L.P., Makeyeva, L.I., Milev, A., Usenko, A.Y., 1992. Global patterns of azimuthal anisotropy and deformations in the continental mantle. Geophys. J. Int. 111, 433–447. https://doi.org/10.1111/j.1365-246X.1992.tb02102.x

Wessel, P., Smith, W.H.F., Scharroo, R., Luis, J., Wobbe, F., 2013. Generic Mapping Tools: Improved Version Released. Eos, Trans. Am. Geophys. Union 94, 409–410. https://doi.org/10.1002/2013EO450001

Wolfe, C., Silver, P., 1998. Seismic anisotropy of oceanic upper mantle: Shear wave splitting methodologies and observations. J. Geophys. Res. Solid Earth 103, 749–771.

Wüstefeld, A., Bokelmann, G., 2007. Null Detection in Shear-Wave Splitting Measurements. Bull. Seismol. Soc. Am. 97, 1204–1211. https://doi.org/10.1785/0120060190

Wüstefeld, A., Bokelmann, G., Barruol, G., Montagner, J.-P., 2009. Identifying global seismic anisotropy patterns by correlating shear-wave splitting and surface-wave data. Phys. Earth Planet. Inter. 176, 198–212. https://doi.org/10.1016/j.pepi.2009.05.006

Wüstefeld, A., Bokelmann, G., Zaroli, C., Barruol, G., 2008. SplitLab: A shear-wave splitting environment in Matlab. Comput. Geosci. 34, 515–528. https://doi.org/10.1016/j.cageo.2007.08.002

Yoshizawa, K., 2014. Radially anisotropic 3-D shear wave structure of the Australian lithosphere and asthenosphere from multi-mode surface waves. Phys. Earth Planet. Inter. 235, 33–48.

https://doi.org/10.1016/j.pepi.2014.07.008

Yoshizawa, K., Kennett, B.L.N., 2015. The lithosphere-asthenosphere transition and radial anisotropy beneath the Australian continent. Geophys. Res. Lett. 42, 3839–3846. https://doi.org/10.1002/2015GL063845

Zhang, S., Karato, S., 1995. Lattice preferred orientation of olivine aggregates deformed in simple shear. Nature 375, 774–777.

Additonal References from the Supporting Information

Debayle, E., Dubuffet, F., Durand, S., 2016. An automatically updated S -wave model of the upper mantle and the depth extent of azimuthal anisotropy. Geophys. Res. Lett. 43, 674–682. https://doi.org/10.1002/2015GL067329

Debayle, E., Kennett, B.L.N., 2000. The Australian continental upper mantle: Structure and deformation inferred from surface waves. J. Geophys. Res. Solid Earth 105, 25423–25450. https://doi.org/10.1029/2000JB900212

Korsch, R.J., Doublier, M.P., 2015. Major crustal boundaries of Australia. https://doi.org/10.4225/25/555C181CC0EAE

Monteiller, V., Chevrot, S., 2010. How to make robust splitting measurements for single-station analysis and three-dimensional imaging of seismic anisotropy. Geophys. J. Int. 182. https://doi.org/10.1111/j.1365-246X.2010.04608.x

Rümpker, G., Silver, P., 1998. Apparent shear-wave splitting parameters in the presence of vertically varying anisotropy. Geophys. J. Int. 135, 790–800.

Silver, P.G., Savage, M.K., 1994. The Interpretation of Shear-Wave Splitting Parameters In the Presence of Two Anisotropic Layers. Geophys. J. Int. 119, 949–963. https://doi.org/10.1111/j.1365-246X.1994.tb04027.x

Vecsey, L., Plomerová, J., Babuška, V., 2008. Shear-wave splitting measurements — Problems and solutions. Tectonophysics 462, 178–196. https://doi.org/10.1016/J.TECTO.2008.01.021